Magnetic Resonance Electrical Impedance Tomography Assessment of Electroporation in Different Complex Structures

Marko Stručić[1], Jessica Genovese[2], Samo Mahnič-Kalamiza[1], Igor Serša[3], Vitalij Novickij[4], Damijan Miklavčič[1] and Matej Kranjc[1]

[1] University of Ljubljana, Faculty of Electrical Engineering, Tržaška c. 25, 1000 Ljubljana, Slovenia
[2] University of Bologna, Department of Agricultural and Food Sciences, P. Goidanich 60, Cesena, Italy
[3] Institut "Jožef Stefan", Jamova cesta 39, 1000 Ljubljana, Slovenia
[4] Institute of High Magnetic Fields, Vilnius Gediminas Technical University, Naugarduko g. 41, 03227 Vilnius, Lithuania
Correspondence: Matej Kranjc, e-mail: matej.kranjc@fe.uni-lj.si

Abstract: *The aim of our study was to investigate the degree of membrane permeabilization by applying Pulsed Electric Field (PEF) treatment to plant food matrices (potato, apple, carrot) using magnetic resonance imaging techniques. The effect of electroporation treatment on T_2 relaxation times was evaluated by comparing the electric field distribution obtained by magnetic resonance electrical impedance tomography with the induced changes of T_2 values. The results provided useful insights into the evaluation of electroporation and suggest that magnetic resonance electrical impedance tomography could be used as an efficient tool to improve the efficacy of electroporation treatments.*

Keywords*: electroporation, PEF treatment, electric field, magnetic resonance imaging, magnetic resonance electrical impedance tomography, food processing.*

1 Introduction

Electroporation or Pulsed Electric Field (PEF) treatment of food is an emerging industrial processing technology with a potential to substitute thermal food processes widely used for juice and valuable compound extraction, food dehydration and biorefinery in addition to improving food stability and guarantee its microbiological safety [1]. PEF treatment utilizes short electric pulses with high amplitude to increase cell membrane permeability or in extreme cases even destroy the cell membrane. It requires moderate energy consumption, can be performed relatively fast, allows for better retention of flavour and colour, and preserves nutritional value of foods [2]. Despite the numerous advantages of PEF treatment, there is still lack of suitable and reliable means of evaluating its effects. To tackle this issue, several researchers reported on the analysis of the current signals during the application of the high-voltage pulses, demonstrating that the dynamics of current can be used as a key characterization feature of tissue electroporation [3], [4]. However, there are limits in obtaining detailed information regarding the detection and quantification of electroporation effects in highly inhomogeneous multicellular systems, with a clear drawback of these results being affected by some phenomena such as spatial averaging of conductivity for example.

Magnetic resonance electric impedance tomography (MREIT) is a method allowing for the reconstruction of electric field distribution during pulse delivery indirectly with use of magnetic resonance imaging (MRI) and numerical post-processing algorithms, thus making it attractive for monitoring and evaluation of electroporation treatment of tissues [5].

Furthermore, magnetic resonance electrical impedance tomography (MREIT) has already been suggested as an effective method for electric field distribution monitoring in the tissue during electroporation treatment of plants [6]. In addition, MREIT was also applied in medical applications of electroporation *in vivo*, such as monitoring of the electric field distribution during electroporation of mouse tumours for prediction of the extent of reversibly [7] and irreversibly electroporated regions [8].

Aim of our investigation was to assess the level of membrane permeabilization in plant tissues after PEF treatment by employing different MRI assessment techniques (MREIT and transversal relaxation time T_2 mapping). Experiments were performed in apple fruit, potato tuber, and carrot taproot tissue since these vegetable matrices exhibit different degrees of complexity and are of high interest to industrial PEF applications.

2 Materials and methods

2.1 Plant tissues

The apples (*Malus domestica*, cv 'Golden Delicious'), potatoes (*Solanum tuberosum*, cv 'Liberta') and carrots (*Daucus carota*, cv 'Danvers') used for this study were purchased at the local market (Ljubljana, Slovenia). From each sample, 26 mm high disks of 30 mm in diameter were manually cut with sharp cork-borer.

2.2 Pulsed Electric Field Treatment

Electroporation treatment of the cylindrically shaped tissue samples was performed using an electric pulse generator lab prototype [9] connected to a pair of self-built needle electrodes inserted into the sample tissue. The electrodes, made of platinum/iridium alloy (Pt/Ir: 90/10 %), had a diameter of 1 mm, and were placed at a center-to-center distance of 10.4 mm. PEF protocol consisted of two sequences of 4 pulses with a duration of 100 µs and with a repetition rate at 5 kHz. For each of the tissues studied the voltage amplitude was adjusted to obtain electric field maps of an acceptable signal-to-noise ratio (i.e. apple 1180 V; potato 750 V; carrot 800 V). The trigger input of the generator was connected to the MRI

spectrometer and synchronized with the Current Density Imaging (CDI) pulse sequence. The delivery of the electric pulses was monitored with an oscilloscope (WavePro 7300A, LeCroy, NY, USA) using a voltage (HVD3605A, LeCroy, NY, USA) and a current probe (AP015, LeCroy, NY, USA).

2.3 Current Density Imaging and Magnetic Resonance Electrical Impedance Tomography

Magnetic Resonance Imaging (MRI) was performed on tissues while applying PEF treatment, according to the method described in [6]. The MRI scanner includes a 2.35 T horizontal bore superconducting magnet with resonant proton frequency of 100 MHz (Oxford Instruments, Abingdon, UK) connected to an Apollo spectrometer (Tecmag, Houston TX, USA) and equipped with microimaging accessories with maximum gradients of 250 mT/m (Bruker, Ettlinger, Germany). During the application of the electrical pulses samples were scanned using the Current Density Imaging (CDI) method to acquire maps of current-induced magnetic field change in the sample [10]. The CDI data combined with the known sample geometry and the potentials at the electrodes, were inputs to the MREIT algorithm to calculate the electric field distribution in the plant tissue. Using the J-substitution algorithm CDI maps were processed to obtain electric field along evaluation line [11].

In this study, the CDI pulse sequence (Fig. 1A) was performed with two acquisitions of relaxation enhancement (RARE) imaging sequence [12], using the following parameters: field of view 30 mm, imaging matrix 64 x 64, inter-echo delay 2.64 ms and slice thickness of 8 mm. In the sequence, electric pulses (Fig. 1B) were delivered between the excitation RF pulse and the first refocusing RF pulse. The MREIT algorithm was solved using the finite element method with the MATLAB 2021b numerical computing environment (MathWorks, Natick, MA, USA) on a desktop PC.

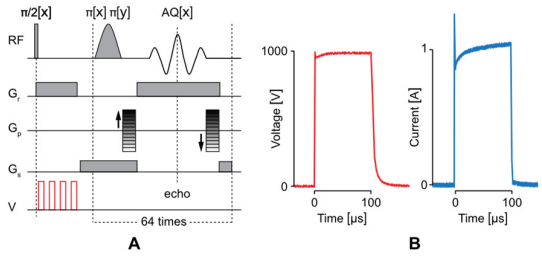

Figure 1: (A) Two-shot RARE CDI sequence that was used to acquire a map of current-induced magnetic field changes. The first part of the sequence – a current encoding part; shows four (100 μs long) high-voltage electric pulses (square pulses represented in the last row) delivered immediately after 90° radiofrequency (RF) excitation pulse. (B) Example of voltage and electric current measurements in one of the representative electric pulses

2.4 *T2* weighted imaging

Plant tissues were monitored with multiparametric MRI consisting of T_2-weighted imaging. A multi-spin-echo (MSE) imaging sequence based on the Carr-Purcell-Meiboom-Gill (CPMG) multi-echo train [13] was chosen to acquire T_2-weighted MR images before and immediately after PEF treatment (i.e. a total of 18 min after pulsation). Following imaging parameters were used: field of view 30 mm; imaging matrix 128 x 128; inter-echo delay 70 ms, slice thickness of 5.1 mm. T_2 maps were calculated using the MRI Analysis Calculator plug-in of ImageJ image processing software (NIH, US), fitting raw MSME data to variable TE (n = 8 echoes) (R^2 > 0.9). For quantitative assessment of the T_2-weighted images MATLAB 2021b (MathWorks, Natick, MA, USA) on a desktop PC was used.

3 Results

In our research study we measured electric field distributions in apple, potato, and carrot samples that underwent PEF treatment. Besides MREIT analysis, T_2 maps before and after treatment were also acquired in the same samples without altering their position to spatially determine redistribution of water inside tissue compartments that would occur due to electroporation. This approach was selected to evaluate the impact of electroporation treatment on transversal relaxation times. In addition, observed changes in T_2 relaxation times were coinciding with specific amplitudes of electric fields, distribution of which was obtained using MREIT technique. Fig. 2 shows examples of T_2-weighted changes, obtained by subtracting voxel value of T_2 map after PEF treatment from corresponding voxel value of T_2 map before PEF treatment, for apple, potato and carrot and T_2 changes with electric field distribution along evaluation line crossing the centre of the sample (see evaluation line on Fig. 2). As can be observed in Fig. 2, general decrease in T_2 relaxation times after PEF treatment was detected in both apple and potato tissues, whereas in carrot tissue, an increase in T_2 values was observed. In apple sample T_2, changes were present across the entirety of the sample, since electric fields throughout the whole apple sample surpassed the threshold electric field for apple tissue (500 V/cm) [4]. In potato tuber and carrot samples we were able to observe changes of T_2 times coinciding with electric fields above 250 V/cm and 200 V/cm respectively, suggesting this value as the threshold electric field for the latter two tissues.

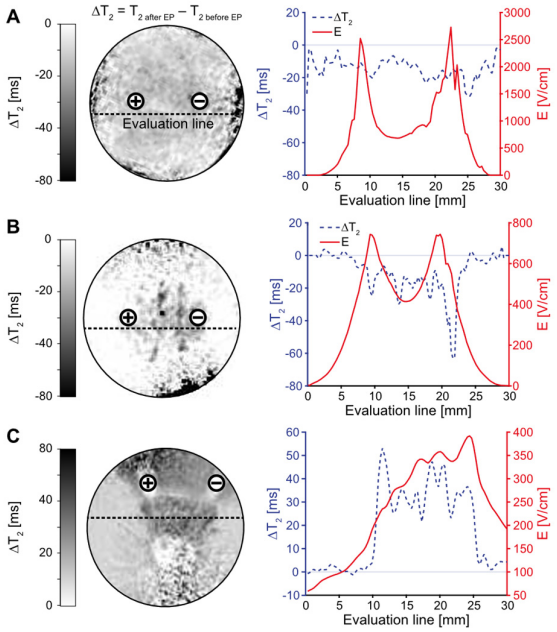

Figure 2. For each of the samples (A) apple, (B) potato tuber and (C) carrot subtraction of T_2-weighted images acquired before and after electroporation treatment (i.e. total imaging time 18 min after the PEF treatment) can be seen on the right side with location of electrodes marked with + and – sign and evaluation line depicted with black dotted line. Respectively, on the left side T_2 differences (dotted line) and electric field (solid line) along the evaluation line are depicted.

4 Discussion

Magnetic resonance imaging has been used previously to monitor spatially-dependent electroporation achieved by PEF treatment in plant tissues [6], [14]. In this study, we assessed electric field distribution and redistribution of water and solutes in the plant tissues by measuring transverse relaxation time T_2 before and after PEF [15]. In fact, the T_2 relaxation value correlates with the proton exchange between water and solutes, as well as with the diffusion of water protons through internally-generated magnetic field gradients by surrounding water protons, leading to differences in the magnetic susceptibility of the tissue exposed to the magnetic field (e.g. at the interfaces between air and fluid-filled pores). Therefore, T_2 values are associated with the structure of the sample based on its water content and water mobility. The overall decrease in T_2 in apple and potato tuber plant tissues due to electroporation could be attributed to the loss of compartmentalization and diffusion of intracellular water and leakage of ions through the tonoplast and plasma membrane, leading to changes in internal morphology (e.g. shrinkage) and different water-solution interactions. On the contrary an increase of T_2 in the carrot's xylem (vascular structure) was observed. Which could be attributed to an increased water flow towards this vascular network of the plant upon water release from cells in carrot's phloem (cortical structure).

The ability of MREIT to monitor local changes due to electroporation is most evident in potato and carrot tissue, where T_2 changes are only visible in areas exceeding the threshold for electroporation (≈ 250 V/cm for potato and ≈ 200 V/cm for carrot xylem). In contrast, changes in water mobility detected in apple tissue using MR imaging encompassed the entire sample. Thus, even though MREIT provided us with information on electric field distribution across the evaluation line, T_2 maps of this tissue show diffuse changes suggesting electroporation thresholds have been excided even in the areas with the lowest electric fields.

5 Conclusions

Monitoring of the electric field distribution during PEF treatment by means of magnetic resonance and electrical impedance tomography is described and experimentally investigated on various complex plant structures. Our research findings provide useful insights into the evaluation of electroporation and suggest that MREIT could be used as an efficient tool in improving and further understanding of PEF treatment in various foods. Since monitoring is performed during pulse delivery, detected electric field distribution considers all heterogeneities and conductivity fluctuations, which occur in the treated tissue. This near-real-time information can also be used for fine tuning of PEF treatment parameters, such as amplitudes of delivered pulses or applying additional pulses, during the PEF treatment, to achieve optimal results. Still, additional research is warranted to investigate the full range of possibilities offered by the MREIT in the field of electroporation.

6 Acknowledgments

This work was supported by the Slovenian Research Agency (research core funding No. P2-0249, funding for Junior Researcher to MS and project No. J2-1733 to MK).

REFERENCES

[1] S. Mahnič-Kalamiza, E. Vorobiev, and D. Miklavčič, "Electroporation in Food Processing and Biorefinery," *The Journal of Membrane Biology*, vol. 247, no. 12, pp. 1279–1304, Dec. 2014, doi: 10.1007/s00232-014-9737-x.

[2] F. J. Barba *et al.*, "Current applications and new opportunities for the use of pulsed electric fields in food science and industry," *Food Research International*, vol. 77, pp. 773–798, Nov. 2015, doi: 10.1016/j.foodres.2015.09.015.

[3] J. Langus, M. Kranjc, B. Kos, T. Šuštar, and D. Miklavčič, "Dynamic finite-element model for efficient modelling of electric currents in electroporated tissue," *Scientific Reports*, vol. 6, no. 1, p. 26409, Sep. 2016, doi: 10.1038/srep26409.

[4] J. Genovese *et al.*, "PEF-treated plant and animal tissues: Insights by approaching with different electroporation assessment methods," *Innovative Food Science & Emerging Technologies*, vol. 74, p. 102872, Dec. 2021, doi: 10.1016/j.ifset.2021.102872.

[5] M. Kranjc, F. Bajd, I. Sersa, and D. Miklavcic, "Magnetic Resonance Electrical Impedance

Tomography for Monitoring Electric Field Distribution During Tissue Electroporation," *IEEE Transactions on Medical Imaging*, vol. 30, no. 10, pp. 1771–1778, Oct. 2011, doi: 10.1109/TMI.2011.2147328.

[6] M. Kranjc, F. Bajd, I. Serša, M. de Boevere, and D. Miklavčič, "Electric field distribution in relation to cell membrane electroporation in potato tuber tissue studied by magnetic resonance techniques," *Innovative Food Science and Emerging Technologies*, vol. 37, pp. 384–390, Oct. 2016, doi: 10.1016/j.ifset.2016.03.002.

[7] M. Kranjc *et al.*, "In Situ Monitoring of Electric Field Distribution in Mouse Tumor during Electroporation," *Radiology*, vol. 274, no. 1, pp. 115–123, Jan. 2015, doi: 10.1148/radiol.14140311.

[8] M. Kranjc, S. Kranjc, F. Bajd, G. Serša, I. Serša, and D. Miklavčič, "Predicting irreversible electroporation-induced tissue damage by means of magnetic resonance electrical impedance tomography," *Scientific Reports*, vol. 7, no. 1, Dec. 2017, doi: 10.1038/s41598-017-10846-5.

[9] V. Novickij *et al.*, "High-frequency submicrosecond electroporator," *Biotechnology & Biotechnological Equipment*, vol. 30, no. 3, pp. 607–613, May 2016, doi: 10.1080/13102818.2016.1150792.

[10] M. Joy, G. Scott, and M. Henkelman, "In vivo detection of applied electric currents by magnetic resonance imaging," *Magnetic Resonance Imaging*, vol. 7, no. 1, pp. 89–94, Jan. 1989, doi: 10.1016/0730-725X(89)90328-7.

[11] Hyun Soo Khang *et al.*, "J-substitution algorithm in magnetic resonance electrical impedance tomography (MREIT): phantom experiments for static resistivity images," *IEEE Transactions on Medical Imaging*, vol. 21, no. 6, pp. 695–702, Jun. 2002, doi: 10.1109/TMI.2002.800604.

[12] I. Serša, "Auxiliary phase encoding in multi spin-echo sequences: Application to rapid current density imaging," *Journal of Magnetic Resonance*, vol. 190, no. 1, pp. 86–94, Jan. 2008, doi: 10.1016/j.jmr.2007.10.009.

[13] H. Y. Carr and E. M. Purcell, "Effects of Diffusion on Free Precession in Nuclear Magnetic Resonance Experiments," *Physical Review*, vol. 94, no. 3, pp. 630–638, May 1954, doi: 10.1103/PhysRev.94.630.

[14] N. Dellarosa, L. Ragni, L. Laghi, U. Tylewicz, P. Rocculi, and M. Dalla Rosa, "Time domain nuclear magnetic resonance to monitor mass transfer mechanisms in apple tissue promoted by osmotic dehydration combined with pulsed electric fields," *Innovative Food Science & Emerging Technologies*, vol. 37, pp. 345–351, Oct. 2016, doi: 10.1016/j.ifset.2016.01.009.

[15] M. Hjouj and B. Rubinsky, "Magnetic Resonance Imaging Characteristics of Nonthermal Irreversible Electroporation in Vegetable Tissue," *The Journal of Membrane Biology*, vol. 236, no. 1, pp. 137–146, Jul. 2010, doi: 10.1007/s00232-010-9281-2.